2008 IEEE International Conference on
Robotics and Automation
Pasadena, CA, USA, May 19-23, 2008

Calibration of Kinematic Parameters of a Car-Like Mobile Robot to Improve Odometry Accuracy

Kooktae Lee and Woojin Chung

Abstract—**Recently, automatic parking assist systems have become commercially available in some cars. In order to improve the reliability and accuracy of parking control, pose estimation problem needs to be solved. Odometry is widely used for pose estimation of a mobile robot. However, most previous odometry calibration methods have focused on two wheeled mobile robots. In this paper, we consider systematic error sources of the Car-Like Mobile Robot(CLMR), and we suggest a useful calibration method for systematic errors. Finally, our calibration method is verified by experiments using a miniature car.**

I. Introduction

RECENTLY, automotive vehicles have become equipped with various intelligent functions. One of the noticeable functions is the parking assist system. Once the driver switches into the parking assist mode from the starting location, the controller generates a target trajectory and controls the EPS (Electronic Power Steering) to reach the target. A translational motion is manually controlled by the driver.

Some problems, however, have to be solved to improve the accuracy and reliability of parking control. One of the significant problems is the accumulated odometry uncertainty during the parking motion. If the odometry accuracy is sufficiently high, then parking control can be carried out using pure odometry, because the travel distance is short.

Odometry contains uncertainties, which are caused by systematic and nonsystematic errors. Systematic errors can be compensated by using a proper calibration method; thus, accuracy can be improved. Most previous researches on systematic error calibration methods have been focused on two wheeled mobile robots. However, there are some works on odometry calibration of the car-like mobile robot(CLMR). Mckerrow and Ratner[1] introduced a systematic error calibration method for CLMR. However, their method, ultrasonic sensors are used as external sensors. Therefore, the calibration range readings of the sensor itself are required additionally. Bonnifait and Bouron[2] researched nonsystematic error reduction methods for CLMR by using odometry redundancy. However, they did not suggest any calibration schemes for systematic errors.

UMBmark[3] suggested the calibration of systematic errors by monitoring the final position of the robot after driving the robot along a pre-programmed path. This skill is simple and practical. However, UMBmark[3] is not directly applicable to CLMR because CLMR can not change its orientation without translational motion. Another great difference between two wheeled mobile robot and CLMR is that the CLMR's wheels can not be controlled independently.

In this paper, we investigate the effects of systematic error sources on odometry and suggest a simple and easy calibration method for systematic errors of CLMR. Finally, we validate our method by experiments.

Manuscript received October 15, 2007.

K. Lee is with Department of Mechanical Engineering, Korea University, Seoul, KOREA (e-mail: hakuna79@ korea.ac.kr).

W. Chung is with Department of Mechanical Engineering, Korea University, Seoul, KOREA (corresponding author to provide phone: 822-3290-3375; e-mail: smartrobot@ korea.ac.kr).

II. Odometry model for CLMR

Systematic error sources, which result in pose errors between the real path and odometry, can be listed as follows.

1) Unequal wheel diameter (each four wheel)
2) Effective wheel base (front and rear wheel)
3) Misalignment of wheels
4) Length between front and rear axle (L)

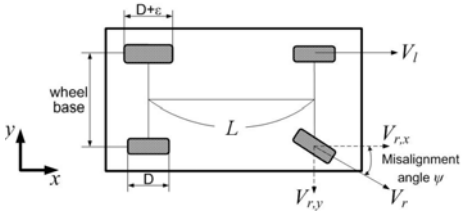

Fig. 1 Systematic error sources for CLMR

It is not easy to consider all systematic error sources for the calibration. Therefore, we concentrate on the dominant systematic error sources. From our experience, we found that the wheel base and wheel diameters are the dominant factors.

Misalignment of wheels also affects odometry accuracy. However, the effect of misalignment can be related to unequal wheel diameters. We assume that the front right wheel misaligned, as shown in Fig.1. The translational velocity of the right wheel V_r is decomposed into two Cartesian coordinate vectors $V_{r,x}$ and $V_{r,y}$. For small misalignment angle ψ, $V_{r,y}$ can be disregarded and the translational velocity can be obtained as $V_{r,x} = V_r \cos\psi$. This equation implies that misalignment ψ "scales" the translational velocity by the factor of cos ψ. With respect to odometry error, we can obtain the same results if the wheel radius is smaller than the nomin al diameter by the factor of cosψ. Therefore, misalignments should not be considered independently.

For the short time period Δt, the robot pose can be computed as follows.

$$\begin{aligned} x_k &= x_{k-1} + \Delta d_r \cdot \cos(\theta_{k-1} + \Delta\theta/2) \\ y_k &= y_{k-1} + \Delta d_r \cdot \sin(\theta_{k-1} + \Delta\theta/2) \\ \theta_k &= \theta_{k-1} + \Delta\theta \end{aligned} \quad (1)$$

$$\Delta d_r = \frac{\Delta d_{rr} + \Delta d_{rl}}{2} \tag{2}$$

$$\Delta\theta = \frac{\Delta d_r}{L}\tan\phi \tag{3}$$

In (2), Δd_{rr} and Δd_{rl} are the incremental displacements of the rear right and left wheels, respectively. L in (3) is the length between the front and rear axle. Generally, the orientation is calculated by (3) for CLMR. However, if there are modeling errors in L or the steering angle Φ, then odometry becomes inaccurate.

$$\Delta\theta = \frac{\Delta d_{rr} - \Delta d_{rl}}{b} \tag{4}$$

Odometry of the two wheeled mobile robot uses (4) in calculating the orientation, where b in (4) is the wheel base. (4) is directly applicable to CLMR. By using (4), the orientation can be easily computed regardless of L or Φ.

The systematic odometry error calibration method, which we propose in this paper, can be applied easily. The test vehicle is driven in an open loop along the pre-programmed path, and then the resultant position is monitored.

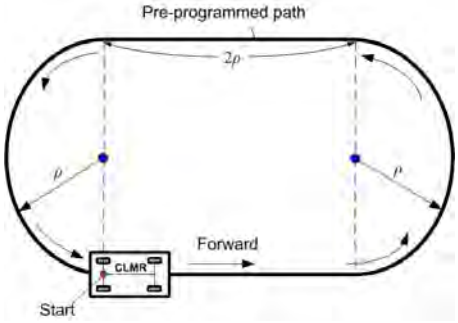

Fig. 2 Pre-programmed path for the calibration of the systematic odometry error

As shown in Fig. 2, after the CLMR's test drive along the pre-programmed path, the dominant systematic error sources (effective wheel base and unequal wheel diameter) can be calibrated by using the differences between the real positions and odometry. The pre-programmed path is set as follows.

1) From the starting position, go straight by the length of 2ρ. (where ρ is the curvature radius of the semicircle which is on both sides of the pre-programmed path)
2) Turn left (or right) with a constant radius of curvature(ρ) while the semicircle is completed.
3) Go straight again by the length of 2ρ.
4) Turn left (or right) with the constant radius of curvature(ρ) while the semicircle is completed.
5) CLMR arrives at the same starting position.

III. Calibration of Systematic Odometry Errors

In practice, both effective wheel base and unequal wheel diameters affect odometry accuracy. However, we consider each factor independently.

A. Type A: uncalibrated wheel base

Type A errors are caused only by the uncalibrated wheel base. We assume that rear wheel diameters are identical and only the wheel base contains an error. When the CLMR moves along the pre-programmed path in the directions CW and CCW, odometry is computed as shown by the dashed line in Fig.3.

Since we assume that rear wheel diameters are identical in Type A errors, odometry and real path are identical in the straight line section. On the other hand, in the semicircle section, the radius of curvature from the odometry data is smaller or larger than the real path because the wheel base is not calibrated.

We assume that the nominal wheel base is smaller than the actual wheel base. As a result, odometry path in the semicircle section is not identical to the real path and we can present this difference by using angle α which is caused by uncalibrated wheel base. This angle α causes the final position error between the real path and odometry. In the CW and CCW directions, the final position (x_4, y_4) can be computed as follows.

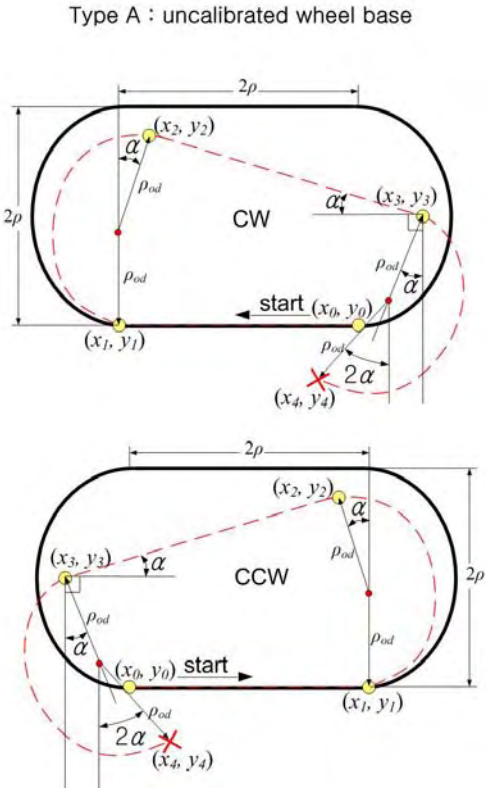

Fig. 3 Type A errors in CW(start at the right bottom) and CCW(start at the left bottom) directions. We assume that the rear wheel diameters are identical and only the wheel base is not calibrated

For Type A Errors in the CW Direction:

$$\begin{aligned}
x_1 &= x_0 - 2\rho \\
y_1 &= y_0 \\
x_2 &= x_1 + \rho_{od}\sin\alpha \approx -2\rho + \rho_{od}\alpha \\
y_2 &= y_1 + \rho_{od} + \rho_{od}\cos\alpha \approx 2\rho_{od} \\
x_3 &= x_2 + 2\rho\cos\alpha \approx \rho_{od}\alpha \\
y_3 &= y_2 - 2\rho\sin\alpha \approx 2(\rho_{od} - \rho\alpha) \\
x_4 &= x_3 - \rho_{od}\sin\alpha - \rho_{od}\sin 2\alpha \approx -2\rho_{od}\alpha \\
y_4 &= y_3 - \rho_{od}\cos\alpha - \rho_{od}\cos 2\alpha \approx -2\rho\alpha
\end{aligned} \tag{5}$$

For Type A Errors in CCW Direction:

$$
\begin{aligned}
x_1 &= x_0 + 2\rho \\
y_1 &= y_0 \\
x_2 &= x_1 - \rho_{od}\sin\alpha \approx 2 \quad - \quad _{od} \quad \rho \quad \rho \quad \alpha \\
y_2 &= y_1 + \rho_{od} + \rho_{od}\cos \quad \approx 2 \quad _{od}\alpha \quad \rho \\
x_3 &= x_2 - 2\rho\cos\alpha \approx - \quad _{od} \quad \rho \quad \alpha \\
y_3 &= y_2 - 2\rho\sin\alpha \approx 2(\quad _{od} - \quad \rho) \quad \rho \quad \alpha \\
x_4 &= x_3 + \rho_{od}\sin\alpha + \rho_{od}\sin 2 \quad \approx 2\alpha_{od} \quad \rho \quad \alpha \\
y_4 &= y_3 - \rho_{od}\cos\alpha - \rho_{od}\cos 2 \quad \approx -2 \quad \rho \quad \alpha
\end{aligned}
\tag{6}
$$

We used mathematical approximations for small angles as follows:

$$
\begin{aligned}
&\sin\alpha \approx \alpha, \sin 2\alpha \approx 2 \quad , \sin 3 \quad \approx 3\alpha \quad \alpha \quad \alpha \\
&\cos\alpha \approx 1, \cos 2\alpha \approx 1, \cos 3 \quad \approx 1 \quad \alpha
\end{aligned}
\tag{7}
$$

Fig.4 shows the right side of Type A errors in the CCW direction. Although the CLMR moves along the semicircle, odometry is presented as a dashed line. The travel distance of the real path and odometry are identical because we assume that rear wheel diameters are equal.

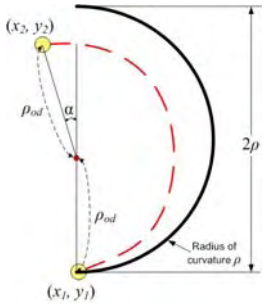

Fig. 4 Length of curve between pre-programmed path and odometry

Therefore, arc length S of the solid line and dashed line are identical and their relations are as follows.

$$
\begin{aligned}
S &= \rho\pi = \rho_{od}(\quad + \quad)\pi \quad \alpha \\
\rho_{od} &= \frac{\pi}{(\pi+\alpha)}\rho
\end{aligned}
\tag{8}
$$

By using (8), the final position of Type A errors in CW and CCW directions can be presented as (9) and (10).

$$
\begin{aligned}
CW: \quad x_4 &= \frac{-2\pi}{(\pi+\alpha)}\rho\alpha \\
y_4 &= -2\rho\alpha
\end{aligned}
\tag{9}
$$

$$
\begin{aligned}
CCW: \quad x_4 &= \frac{2\pi}{(\pi+\alpha)}\rho\alpha \\
y_4 &= -2\rho\alpha
\end{aligned}
\tag{10}
$$

B. Type B: uncalibrated wheel diameter

Secondly, we consider the case which the effective wheel base is calibrated and rear wheel diameters contain the modeling error. We call this case as Type B. In Fig.5, we assume that the rear left wheel diameter is slightly larger than the rear right wheel diameter. Then, odometry shows a curved path in the straight line section, and angle β is shown in Fig.5.

Also, in the semicircle section, odometry is not identical to the real path in the CW and CCW direction. The magnitude of this angle is presented as γ. The final position of Type B errors could be derived similarly as Type A errors.

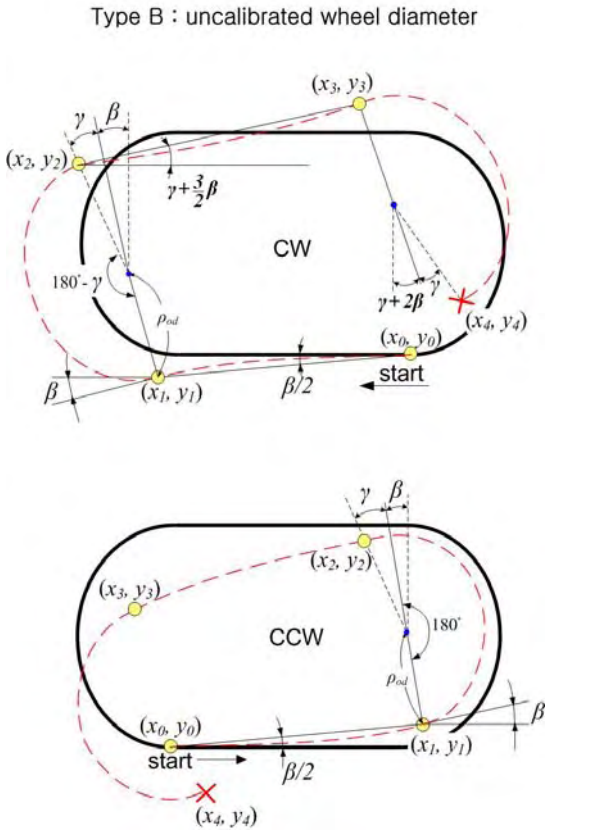

Fig. 5 Type B errors in CW(start at the right bottom) and CCW(start at the left bottom) directions. The effective wheel base is assumed to be known, and rear wheel diameters are assumed to contain the modeling error.

For Type B Errors in the CW Direction:

$$
\begin{aligned}
x_1 &= x_0 - 2\rho\cos(\beta/2) \approx -2\rho \\
y_1 &= y_0 - 2\rho\sin(\beta/2) \approx -\rho\beta \\
x_2 &= x_1 - \rho_{od,CW}\sin\beta - \rho_{od,CW}\sin(\beta+\gamma) \\
y_2 &= y_1 + \rho_{od,CW}\cos\beta + \rho_{od,CW}\cos(\beta+\gamma) \\
x_3 &= x_2 + 2\rho\cos(3\beta/2+\gamma) \\
y_3 &= y_2 + 2\rho\sin(3\beta/2+\gamma) \\
x_4 &= x_3 + \rho_{od,CW}\sin(2\beta+\gamma) + \rho_{od,CW}\sin(2\beta+2\gamma) \\
y_4 &= y_3 - \rho_{od,CW}\cos(2\beta+\gamma) - \rho_{od,CW}\cos(2\beta+2\gamma)
\end{aligned}
\tag{11}
$$

For Type B Errors in CCW Direction:

$$
\begin{aligned}
x_1 &= x_0 + 2\rho\cos(\beta/2) \approx 2\rho \\
y_1 &= y_0 + 2\rho\sin(\beta/2) \approx \rho\beta \\
x_2 &= x_1 - \rho_{od,CCW}\sin\beta - \rho_{od,CCW}\sin(\beta+\gamma) \\
y_2 &= y_1 + \rho_{od,CCW}\cos\beta + \rho_{od,CCW}\cos(\beta+\gamma) \\
x_3 &= x_2 - 2\rho\cos(3\beta/2+\gamma) \\
y_3 &= y_2 - 2\rho\sin(3\beta/2+\gamma)
\end{aligned}
\tag{12}
$$

$$x_4 = x_3 + \rho_{od,CCW}\sin(2\beta+\gamma) + \quad _{od,CW}\rho\sin(2 \quad +2 \quad)\beta \qquad \gamma$$
$$y_4 = y_3 - \rho_{od,CCW}\cos(2\beta+\gamma) - \quad _{od,CW}\rho\cos(2 \quad +2 \quad)\beta \qquad \gamma$$

The final positions of (11) and (12) can be summarized as follows.

$$CW: \quad x_4 = 2\rho_{od,CW}(\beta+\gamma) \qquad (13)$$
$$y_4 = 2\rho(\beta+ \quad)\gamma$$

$$CCW: \quad x_4 = 2\rho_{od,CCW}(\beta+\gamma) \qquad (14)$$
$$y_4 = -2\rho(\beta+ \quad)\gamma$$

ρ_{od} in (13) and (14) is the radius of curvature by odometry in the semicircle section. Strictly speaking, in the semicircle section with Type B errors, the travel distance obtained from odometry and the real travel distance are not identical. However, we assume that the inequality of wheel diameters is acceptably small compared with the length of the semicircle section. Therefore, a following approximation is adopted.

$$\rho_{od,CW}(\pi-\gamma) \approx \qquad \rho \quad \pi \qquad (15)$$
$$\rho_{od,CCW}(\pi+\gamma) \approx \qquad \rho \quad \pi$$

Also, angle γ is related with β by the following equation. The proof is given in APPENDIX.

$$\gamma = \frac{\pi}{2}\beta \qquad (16)$$

By using (13) ~ (16), the final position (x_4, y_4) is presented as follows.

$$CW: \quad x_4 = \frac{2(2+\pi)}{2-\beta}\rho\beta \qquad (17)$$
$$y_4 = (2+\pi)\rho\beta$$

$$CCW: \quad x_4 = \frac{2(2+\pi)}{2+\beta}\rho\beta \qquad (18)$$
$$y_4 = -(2+\pi)\rho\beta$$

In practice, Type A and Type B errors occur at the same time. Therefore, we apply the superposition in the CW and CCW directions.

$$CW: \quad x_{c.g,CW} = \frac{-2\pi}{\pi+\alpha}\rho\alpha + \frac{2(2+\pi)}{2-}\rho_{\beta} \qquad \beta \qquad (19)$$

$$CCW: x_{c.g,CCW} = \frac{2\pi}{\pi+\alpha}\rho\alpha + \frac{2(2+\pi)}{2+}\rho_{\beta} \qquad \beta$$

Finally, (19) is rearranged by α and β as follows.

$$\alpha = \frac{-\pi(x_{c.g.,CW} - x_{c.g.,CCW})}{x_{c.g.,CW} - x_{c.g.,CCW} + 4\pi\rho} \qquad (20)$$

$$\beta = \frac{-1+\sqrt{1+[(x_{c.g.,CW}+x_{c.g.,CCW})/2(2+\pi)\rho)]^2}}{(x_{c.g.,CW}+x_{c.g.,CCW})/4(2+\pi)\rho} \qquad (21)$$

Moreover, α and β can be presented by using y -direction as follows.

$$CW: y_{CW} = -2\rho\alpha + (2+\pi) \quad = y_{c.g.,CW} \quad \rho \qquad \beta \qquad (22)$$
$$CCW: y_{CCW} = -2\rho\alpha - (2+\pi)\rho\beta = y_{c.g.,CCW}$$

$$\alpha = \frac{y_{c.g.,CW} + y_{c.g.,CCW}}{-4\rho} \qquad (23)$$

$$\beta = \frac{y_{c.g.,CW} - y_{c.g.,CCW}}{2(2+\pi)\rho} \qquad (24)$$

In theory, α's from (20) and (23) should be identical. In the same way, β's from (21) and (24) should be also identical. From these derived angles α and β, we can calibrate the wheel base and unequal wheel diameters. The relation between angle α and wheel base b is given by (25). If the nominal value of the wheel base is smaller than the effective wheel base, α is negative. On the other hand, if the nominal value is larger than the effective wheel base, α is positive.

$$\frac{b_{actual}}{\pi} = \frac{b_{nominal}}{\pi-\alpha} \qquad (25)$$

Also, we can calculate the ratio between the rear right and left wheels and it can be derived from the geometric relation in Fig.6.

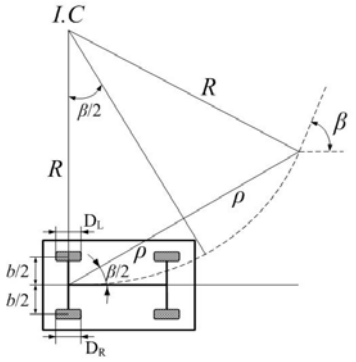

Fig. 6 Geometric relation for the radius of curvature

As shown in Fig.6, the dashed curve has an instantaneous center at I.C. , and the radius of curvature R is presented as (26).

$$R = \frac{\rho}{\sin(\beta/2)} \qquad (26)$$

Also, the ratio of the rear wheel diameters can be derived as follows.

$$\frac{D_R}{D_L} = \frac{R+b/2}{R-b/2} \qquad (27)$$

IV. Steering Angle Calibration Experiments

CLMR used in experiments are shown in Fig.7. This CLMR has the same kinematic structure as the car-like vehicle.

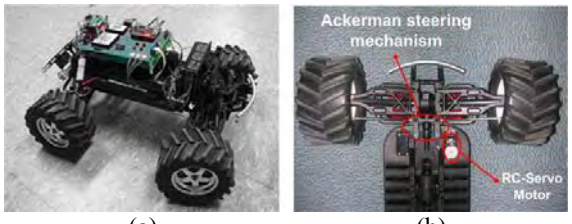

(a) (b)

Fig. 7 (a) Car-Like Mobile Robot used in experiments (b) Bottom side of CLMR – Front wheels have Ackerman steering mechanism

According to the ground contact conditions, the resultant moving direction may not coincide with the steering angle command. Therefore, steering angle calibration is carried out first. Fig. 8 shows traces of the model car, which were obtained by using a camera when the steering angle was fixed. A steering angle changes from 20.6° to -19.7°, which are the joint limits. In calibration experiments, a steering angle was incrementally increased by 0.4 degrees.

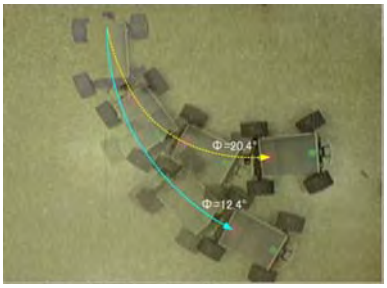

Fig. 8 Calibration Experiments for steering angles for only two steering inputs when ϕ =12.4°, 20.4°

From the arc traces of the model car, the result which was obtained by applying the least square method for the circle fitting [4] is shown in Fig. 9-(a). After the center of the circle and the radius of curvature are computed, the steering angle ϕ can be calibrated.

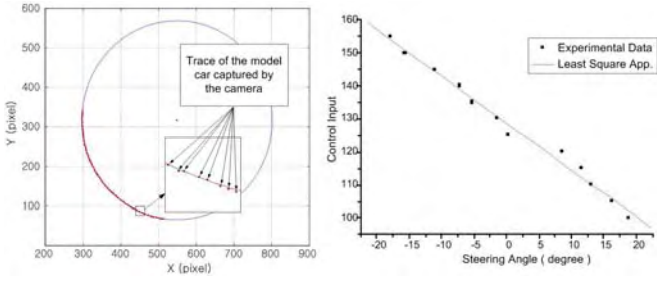

(a) (b)

Fig. 9 (a) Least Square Method for Circle fitting (total 120 data when the steering angle was 12. 4°) (b) Least Square linear approximation of steering angle - input value

Experiments were carried out for all ranges of the steering angle. The relations between the steering angle and the control input are obtained. As shown in Fig. 9-(b), a least square approximation is carried out for data fitting.

V. Experimental Results

Fig.10 shows the experimental results before the calibration. CLMR moved along the pre-programmed path. In the experiments, not only the systematic error sources but also the nonsystematic error sources result in odometry errors Therefore, we obtained the center of gravity after 5 experiments for the CW and CCW directions. By using the center of gravity, the effects of nonsystematic error can be averaged.

Before the calibration, the nominal wheel base and wheel diameter ratio were b = 30cm and D_R/D_L=1.00(D_R= D_L =9cm) respectively. After applying our calibration method using the resultant position, we obtained b = 28cm and D_R/D_L = 0.99. Finally, to confirm the calibration, we drove CLMR along the pre-programmed path again and results are also shown in Fig.10.

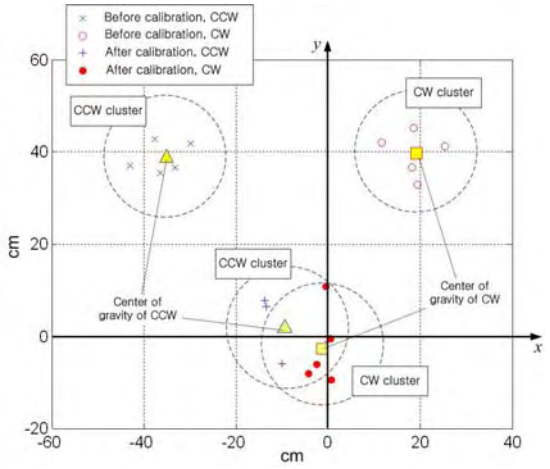

Fig. 10 Experimental results after calibration; Before calibration: b = 30cm, D_R/D_L = 1.00; After calibration: b = 28cm, D_R/D_L = 0.99

In order to evaluate performances, resultant positional error is used. The absolute offset of the two centers of gravity from the origin are denoted by $r_{c.g.,CW}$ and $r_{c.g.,CCW}$ as follows.

$$r_{c.g.,CW} = \sqrt{(x_{c.g.,CW})^2 + (y_{c.g.,CW})^2} \quad (28)$$

$$r_{c.g.,CCW} = \sqrt{(x_{c.g.,CCW})^2 + (y_{c.g.,CCW})^2} \quad (29)$$

Table I Systematic error calibration results

Experiment	Before calibration $E_{max,syst}$[cm]	After calibration $E_{max,syst}$[cm]	Improvement	Before calibration	After calibration	Comment	Figure (front) (rear)
1	52.9	9.6	5.5 times	b = 30cm D_R/D_L=1.00	b = 28cm D_R/D_L=0.99	Details are shown in Fig.10 and Fig.11	
2	196.8	12.7	15.5 times	b = 30cm D_R/D_L=1.00	b = 30cm D_R/D_L=1.07	Increase of 3% rear right wheel diameter by winding tape	
3	159.8	16.7	9.6 times	b = 30cm D_R/D_L=1.00	b = 27cm D_R/D_L=0.96	Increase of 3% rear left wheel diameter by winding tape	
4	91.5	8.9	10.3 times	b = 30cm D_R/D_L=1.00	b = 27cm D_R/D_L=0.96	Winding tape around left outside of rear left and right wheels	

The larger value between $r_{c.g.,CW}$ and $r_{c.g.,CCW}$ is the measure of the odometric accuracy for systematic errors.

$$E_{\max,syst} = \max(r_{c.g.,CW}; r_{c.g.,CCW}) \quad (30)$$

As pointed out in [3], the worst case error is our major concern. For further verification, we carried out other experiments. In experiment #2 of Table I, the diameter of the rear right wheel was increased by 3% by intentionally winding a tape around the outer surface of a tire. In experiment #3 of Table I, the diameter of the rear left wheel was increased by 3% by intentionally winding a tape around the outer surface of a tire. In experiment #4, we wound the tape around left outside rear wheels to change effective wheel base. From Table I, it is clear that the resultant positioning accuracy is sufficiently high for all experiments. Regardless of the kinematic parameter changes, our calibration scheme provided accurate results.

The experiments verified that the proposed method can be used to calibrate the systematic odometry error properly.

VI. Conclusion

In this paper, we suggested a systematic error calibration method for CLMR. The proposed method is simple and easy to apply. We validated our method through experiments.

Appendix

For Type B errors, we assume that the rear left wheel diameter is slightly larger than the rear right wheel by ε. Then, angle β, which occurs after driving CLMR along the straight line section, can be presented as follows by using the pulses summation of each wheel encoder and orientation equation (4).

- Straight line section -

$$\theta_{real} = \frac{1}{b}\left[\frac{\pi D \cdot N_R}{C_e} - \frac{\pi(D+\varepsilon)\cdot N_L}{C_e}\right] = 0 \quad (31)$$

$$\theta_{odometry} = \frac{1}{b}\left[\frac{\pi D \cdot N_R}{C_e} - \frac{\pi D \cdot N_L}{C_e}\right] \quad (32)$$

$$\beta = \theta_{real} - \theta_{odometry} = \frac{1}{b}\left[\frac{-\pi\varepsilon \cdot N_L}{C_e}\right] \quad (33)$$

Where,

D : nominal diameter of rear wheels

ε : slightly larger magnitude than nominal wheel diameter

$N_{R(L)}$: pulses summation of rear right(left) wheel for the straight line section(length=2ρ)

C_e : encoder resolution

In the semicircle section, there are differences in pulses of the rear wheels from the straight line section. In the CW direction, left wheel has more pulses than N_L by δ and right wheel has less pulse than N_R by δ.

Also, the ratio of the length between the straight line section(2ρ) and semicircle section($\pi\rho$) is $\pi/2$. This ratio is multiplied to (31) and (32) for computing the orientation of the semicircle section. Angle γ is computed as angle β.

- Semicircle Section -

$$\theta_{real} = \frac{\pi}{2}\cdot\frac{1}{b}\left[\frac{\pi D \cdot (N_R - \delta)}{C_e} - \frac{\pi(D+\varepsilon)\cdot(N_L+\delta)}{C_e}\right] \quad (34)$$

$$\theta_{odometry} = \frac{\pi}{2}\cdot\frac{1}{b}\left[\frac{\pi D \cdot (N_R - \delta)}{C_e} - \frac{\pi D \cdot (N_L+\delta)}{C_e}\right] \quad (35)$$

$$\gamma = \theta_{real} - \theta_{odometry} = \frac{\pi}{2}\cdot\frac{1}{b}\left[\frac{-\pi\varepsilon\cdot(N_L+\delta)}{C_e}\right] = \frac{\pi}{2}\left(\beta - \frac{\pi\varepsilon\delta}{bC_e}\right) \quad (36)$$

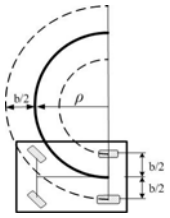

When we drive CLMR along the semicircle path as shown in the left figure, the travel distance of the rear right and left wheels is computed by the following equation.

$$\text{Right: } (\rho - \frac{b}{2})\pi = \frac{\pi}{2}\left[\frac{\pi D\cdot(N_R-\delta)}{C_e}\right] \quad (37)$$

$$\text{Left: } (\rho + \frac{b}{2})\pi = \frac{\pi}{2}\left[\frac{\pi(D+\varepsilon)\cdot(N_L+\delta)}{C_e}\right] \quad (38)$$

Then, we subtract (38) from (37) and we can obtain the following equation.

$$-\pi b = \frac{\pi}{2}\cdot\frac{\pi}{C_e}\left[D\cdot N_R - (D+\varepsilon)\cdot N_L - (2D+\varepsilon)\cdot\delta\right] \quad (39)$$

However, in (39), the term $D\cdot N_R - (D+\varepsilon)\cdot N_L$ is zero because there is no orientation change in the straight line section as presented in (31). Therefore, (39) is rearranged as follows.

$$\delta = \frac{2b}{\pi}\cdot\frac{C_e}{2D+\varepsilon} \quad (40)$$

Finally, (36) is presented as follows by using (40).

$$\gamma = \frac{\pi}{2}\left(\beta - \frac{2\varepsilon}{2D+\varepsilon}\right) \quad (41)$$

However, ε is acceptably small value with respect to the nominal wheel diameter. Therefore, we assume that the value of ε/D is zero. Then, we can obtain γ as follows.

$$\gamma = \frac{\pi}{2}\beta \quad (42)$$

Acknowledgment

This research was supported by Mando Corporation as a part of Parts and Materials Development Project "Vision -based Intelligent Steering System" (VISS)

References

[1] Philip J. Mckerrow and Danny Ratner, "Calibrating a 4-wheel mobile robot", *IEEE/RSJ Intl. Conference on Intelligent Robots and Systems,* 2002.

[2] Philippe Bonnifait and Pascal Bouron, "Data Fusion of Four ABS Sensors and GPS for an Enhanced localization of Car-like Vehicles", *IEEE International Conference on Robotics & Automation*, 2001

[3] J. Borenstein and L. Feng, "Correction of Systematic Odometry Errors in Mobile Robots", *IEEE International Conference on Intelligent Robots and Systems*, pp. 569-574, 1995.

[4] Celestino A. Corral, "On Implementing K°asa's Circle Fit Procedure", *IEEE trans. on instrumentation and measurement,* Vol.47, No.3, 1998.